International Journal of Engineering Trends and Technology
ISSN: 2231 – 5381 /doi:10.14445/22315381/IJETT-V70I1P201

Volume 70 Issue 1, 1-7, January, 2022


*Original Article*

# Kinematic and Dynamic Study of Cam Mechanisms for Bottling Machines

Fabio Corradini[1], Marco Silvestri[2]

[1]*Department of Engineering and Architecture, University of Parma, Parma, Italy*

[2]*Department of Innovative Technologies, SUPSI, Lugano, Switzerland*

[2]marco.silvestri2@unipr.it,[1]fabio.corradini@unipr.it

***Abstract*** *- The main objective of this study is to analyze and optimize the cam mechanisms of the cork capper station currently in use for wine bottling machines. For each machine model considered, current cam profiles and corresponding real trajectories performed during operation are analyzed. Subsequently, various alternative laws of motion are tested to implement the same process, respecting the same precision points but modifying other parts of trajectory to improve machine dynamic performances. A series of tests carried out on a reconfigurable prototype and using different types of cork have made it possible to verify the effectiveness of the new laws of motion and to obtain the load acting on the machine at different operating speeds.*

**Keywords** — *Cam mechanisms, the law of motion, kinematic analysis, dynamic analysis.*

## I. INTRODUCTION

Cam mechanisms are those mechanisms in which the transmission of motion occurs by contact of two specially shaped profiles to achieve the transformation required by the law of motion, i.e., to generate a specific joint trajectory starting from a constant speed rotating shaft.

Usually, they consist of a driving element that moves with uniform rotational motion and of a follower element that moves of reciprocating motion; in particular, if the follower moves with a rectilinear translational motion, it is called tappet, while if it is animated by motion rotatory it is called rocker [1].

Cam mechanisms are very well suited for those machines that must repeatedly perform a series of identical movements. The advantages they offer over other rigid automation systems are freedom in determining motion laws and the relatively simple possibility of replacement if changes must be made. Industrial corking machines fit perfectly in this scenario, and indeed they are often equipped with cam mechanisms to drive three main elements, as illustrated in the following paragraph.

### *A. Corking Machine Operation*

The corking machine performs the capping process through the control of three actuators. In traditional systems, each of these is controlled by a cam connected to the main shaft; this ensures the synchronization of the motion between the axes and the mainline [2]. The systems controlled by their respective cams are:

- the bottle tray cylinder. It performs a vertical movement in order to bring the bottle closer to the plunger and balance its thrust through a preloaded spring.
- The cork plunger. This device also features a vertical motion. Its purpose is to push the cork into the mouth of the bottle.
- The slide of the compression mechanism. This mechanism is made of 4 jaws that compress the cork in order to facilitate its insertion in the bottle. The compression force is regulated by the corresponding cam and by a preloaded spring.

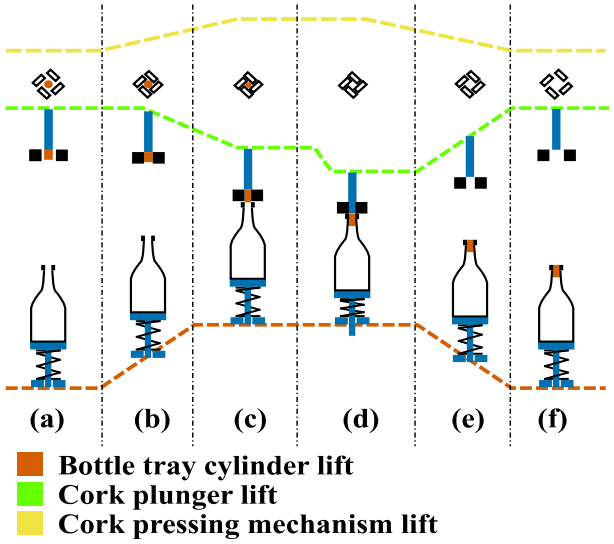


**Fig. 1: Schematic representation of the corking process.**

Fig. 1 shows the schematic representation of the capping phases [3]. A dotted line shows the lifts corresponding to the cams of the three main organs. The process has been schematized in 6 phases.

- Phase 1 (Fig. 1a): The bottle is fed into the machine, the cylinder is lowered, the plunger is raised, and the slide is positioned to keep the jaws open around the cap.
- Phase 2 (Fig. 1b): the axes are moved to the position where the cork is inserted. The bottle tray cylinder is raised, the plunger is lowered, and the slide begins to close the jaws.
- Phase3 (Fig 1c): The cylinder reaches its maximum height, the plunger pushes the cork down to the mouth of the bottle, the jaws compress the cork until it reaches the required size for insertion.
- Phase 4 (Fig. 1d): the cork is inserted. The plunger is completely lowered and pushes the cork into its seat; at the end of this phase, the jaws of the compression mechanism start opening to prevent the cork from getting stuck.
- Phase 5 (Fig 1e): The organs return to their initial position to begin a new cycle.
- Phase 6 (Fig. 1f): the organs have returned to their initial position; as soon as the corked bottle is unloaded and the new cork is placed between the jaws, the working cycle can start again.

### *B. Current Configuration Issues*

In the configuration currently in use on most machines, the cams are made with circular arcs that produce the laws shown in the first graph of Fig. 2.

This kind of solution has the main drawback of very high acceleration peaks related to the speed changes of the axes (third graph in Fig. 2), resulting in excessive vibrations when the machine operates at high speeds [4]. Such vibrations are detrimental to the mechanisms [5], affect the precision of assembly [6], and are a source of noise [7].

The solution here discussed consists of creating a polynomial law that, keeping the machine operation unchanged, smooths down the accelerations at the peaks detected in the experimental phase [8]. Subsequently, a series of tests have been carried out, with the help of a specially made prototype, to verify the effectiveness of the new laws [9]. During these tests, the operation of different types of machines has been simulated, considering the use of different models of cork stoppers to verify the force required to the compression system (the one subjected to the greatest loads).

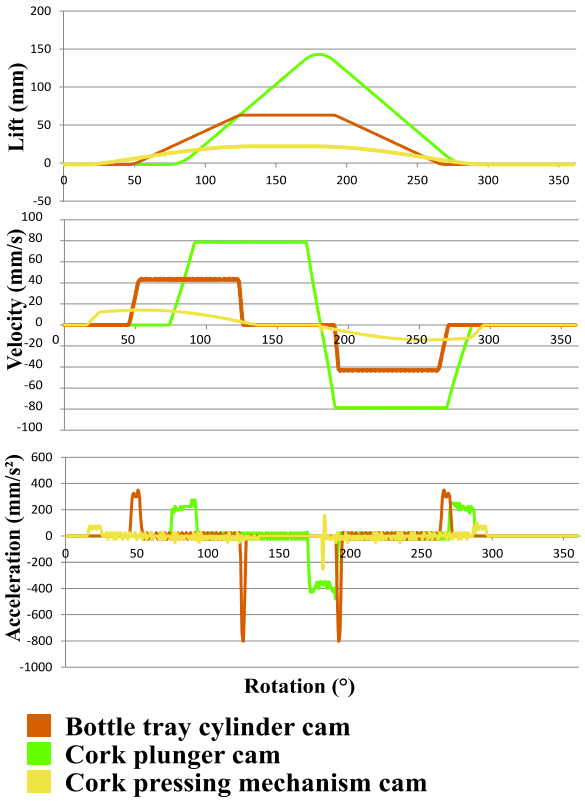


**Fig. 2: Cam lift graph for the MACHINE A. Speed and acceleration data were taken from the test system PLC while the machine was operating at a rate of 500 parts per hour.**

## II. MATERIAL AND METHODS

### *A. Tested Layouts*

Various types of corking machines, characterized by different construction layouts and with different production rates, were considered for the execution of the tests [10] [11]. Corking machines are mainly divided into two categories: single-head machines, which have a single capping head, and rotary machines, which include several capping heads, but other kinematic designs can be found on the market, as described below.

In single-head machines, the cams rotate together with the column, while in the rotary machines, the cams are fixed to the frame, and the remaining mechanical parts (pistons, cylinders, etc...) rotate around them.

In every case, the movement of the parts is imposed through a rigid kinematic mechanism (in most cases through cams) that provides only limited possibilities of adjustment.

The table below shows the characteristics of the machines tested:

| Machine | Layout | Working rate range (Pieces per hour) | Testing rate (Pieces per hour) |
|---|---|---|---|
| MACHINE A | rotary | 500-1500 | 500 |
| MACHINE B | rotary | 400-1600 | 500 |
| MACHINE C | rotary | 500-1500 | 500 |
| MACHINE D | single-head | 1000-3000 | 1000 |
| MACHINE E | single-head | 1400-3500 | 1400 |
| MACHINE F | single-head | 1400-3500 | 1400 |

The only machines, among those considered for the test, whose movement is not entirely controlled by cams are:

- The MACHINE D uses a crankshaft system to move the plunger and a splined shaft to drive the slide of the compression mechanism.
- The MACHINE E uses a crankshaft to move the plunger.

From each of the reported machines, the law of motion of the parts was extrapolated. Next, a polynomial law was determined that could perform the same motion more smoothly but with the same accuracy. As a final step, the polynomial laws of motion of each machine were tested for effectiveness on the prototype machine.

### *B. The polynomial law of motion*

In order to optimize the imposed trajectory of the existing cams, it was decided to replace the circular arcs that defined the original profiles with fifth-degree polynomials, with the objective of maintaining, for each law of motion, the same working lifts and the same operating speeds of the original trajectory [12]. First, for each cam, the fixed working points for which the polynomial law must mandatorily pass to be effective are identified. These must be stationary points, i.e., characterized by zero acceleration and zero velocity. The law of cam motion is then divided into several intervals at the working points just found. Each interval is modeled with a fifth-degree polynomial. Given a law of motion, that is section of the main trajectory and defined in the time range $[t_i, t_f]$, with $q_i$ initial position, $q_f$final position, and $T = t_f - t_i$, it is possible to define a polynomial passing through initial and final points with the following formula [13]:

$$q(t) = a_0 + a_1(t - t_i)^3 + a_2(t - t_i)^4 + a_3(t - t_i)^5$$

$$a_0 = q_i$$

$$a_1 = \frac{20\,(q_f - q_i)}{2T^3}$$

$$a_2 = -\frac{30\,(q_f - q_i)}{2T^4}$$

$$a_3 = \frac{12\,(q_f - q_i)}{2T^5}$$

The law of motion thus formulated is able to smoothly connect two stationary points and ensures continuity of the various segments up to the level of acceleration.

The example of the law of motion of the bottle-holder cylinder for the MACHINE-A(shown in Fig. 1) is given below. In this case, the trajectory was split into five sections delimited by six working points:

| Point | Rotation (°) | Corresponding time at a rate of (500 Pieces per hour) | Cam lift [mm] |
|---|---|---|---|
| 0 | 0 | 0 s | 0 |
| 1 | 45 | 0.9 s | 0 |
| 2 | 125.18 | 2.5 s | 64.83 |
| 3 | 189.81 | 3.8 s | 64.83 |
| 4 | 270 | 5.4 s | 0 |
| 5 | 360 | 7.2 s | 0 |

The polynomial law is then defined for each section. In this way, it is assured the passage for every working point (fig 3).

The table shows the coefficients relative to the polynomial trajectories, assuming the constant movement of the machine at a speed of 500 pieces per hour.

| Sect. | $a_0$ | $a_1$ | $a_2$ | $a_3$ |
|---|---|---|---|---|
| 0 | 0 | 0 | 0 | 0 |
| 1 | 0 | 157.22 | -147.06 | 36.68 |
| 2 | 64.83 | 0 | 0 | 0 |
| 3 | 64.83 | -157.16 | 146.99 | -36.66 |
| 4 | 0 | 0 | 0 | 0 |

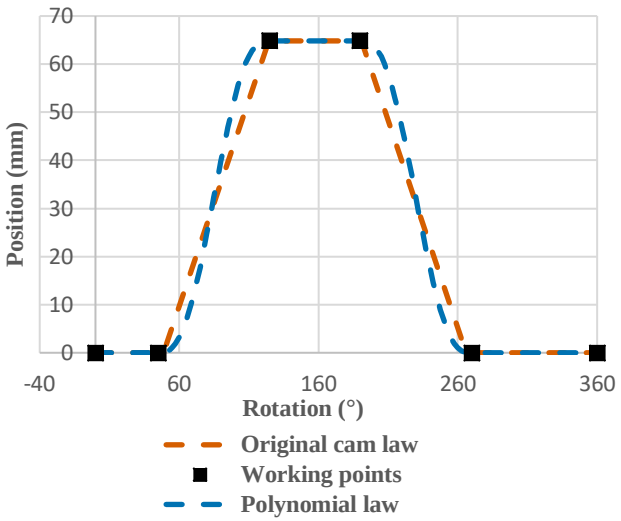


**Fig. 3: the law of motion imposed by the cam of the bottle tray cylinder in the MACHINE-A.**

A comparison between the motion law of the MACHINE-A bottle tray cylinder and the new polynomial law is shown in Fig. 3. It can be seen that the transition for the working points is always respected.

### *C. Practical operation tests*

After designing the new trajectories based on polynomial curves, a set of experimental tests have been carried out on a test machine with a twofold purpose.

In the first place, such tests provide a practical verification of the machine's proper functioning in real operating conditions. Secondly, they allow measuring the maximum load exerted on the system to verify the correct sizing of the motor (and its torque in particular), which is essential to ensure that the motor will actually be able to operate the machine keeping the input speed to the cam mechanisms constant.

More than a thousand tests were performed using the configurations of all the machines, at the minimum and maximum speeds, and with different types of caps [14]. For each test, the dimensions of the caps before and after compression were measured, as well as the force exerted by the compression system during the capping process. The latter value allows determining the maximum resistant torque applied by the load during the operation cycle, and hence the corresponding curves have been reported.

The table shows the caps used for the test:

| **Cork Name** | **Type** |
|---|---|
| Cork_01 | Synthetic cork |
| Cork_02 | Coated synthetic cork |
| Cork_03 | Coated synthetic cork |
| Cork_04 | Natural cork |
| Cork_05 | Twin-top cork |
| Cork_06 | Natural cork |
| Cork_07 | Natural cork |
| Cork_08 | Agglomerate cork |
| Cork_09 | Champagne cork |

The characteristics of the plugs used are briefly explained below[15]:

- Synthetic cork: this is the material used for the cheapest caps, made by extrusion. It is made of a rubbery polymeric compound which has some advantages over the natural cork, such as chemical and microbiological inertia, correct gas transpiration, and homogeneity of physical characteristics [16].
- Coated synthetic cork: itis essentially synthetic cork, but it is of higher quality having a coating that improves its technical characteristics
- Natural cork: it is the classic cork made of the bark of the cork trees. It is suitable for the closure of wines that do not develop too much pressure but, being a natural product, the homogeneity of its physical characteristics is not guaranteed.
- Agglomerated, Twin-top, and Champagne: agglomerated cork is composed of compressed and glued cork chips; it is used in order to have constant technical performances. In the case of the twin-top, two rods of natural cork are placed at the ends to optimize gas permeability[17]. In the case of champagne cork stoppers, the rods are placed at the lower end while the upper end has the classic mushroom shape.

### *D. The Corking Test Machine*

For the test phases, a specially designed corking machine prototype was used, which allows to freely set the laws of motion for the three main systems (bottle tray cylinder, plunger, compression block slide). The test capper, in fact, does not control the motion through cams but is equipped with three independent linear actuators controlled by a driver and a PLC. The actuators have been programmed as "electronic cams," so they move synchronized with a master axis (in this case virtual) that simulates the main axis of the machine, but their motion profile is entirely set via software.

The system is also equipped with a load cell connected to the slider of the compression mechanism to measure the force exerted by the mechanism itself [18].

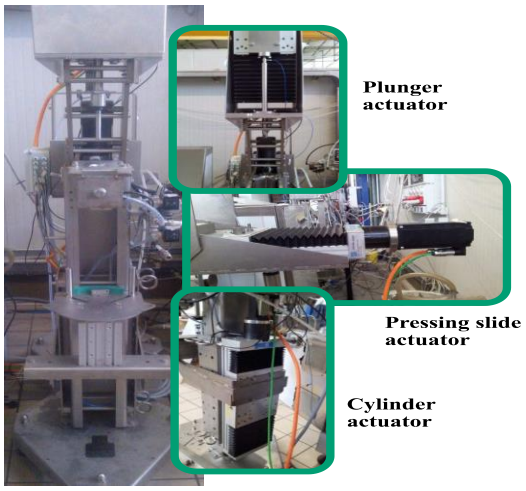


**Fig. 4: The figure shows the prototype used for testing highlighting the actuators.**

Maximum load measurements were reported for each cap type. The plots of the polynomial law of motion and load for the compression system for each machine and cap type at maximum and minimum speeds are also reported.

## III. RESULTS AND DISCUSSION

### *A. Laws of motion and accelerations*

The original laws of motion of the cams for each type of machine and the new polynomial laws are given. For each law, the corresponding accelerations are also given so that a comparison can be made [19].

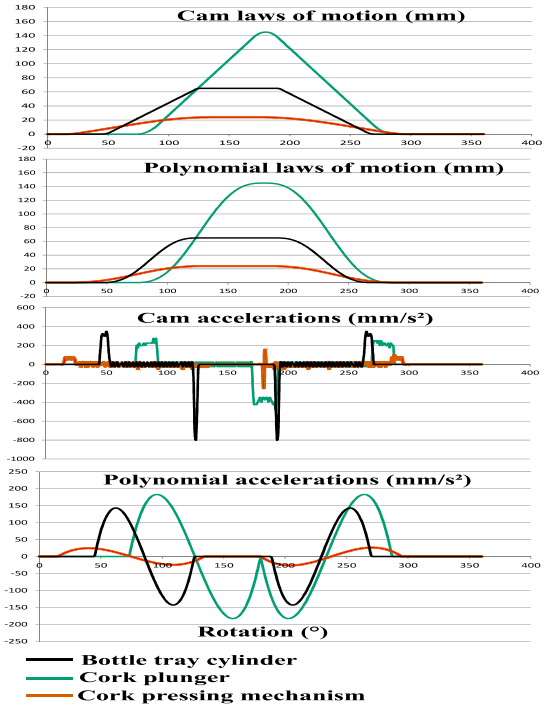


**Fig. 5: Curves of positions and accelerations for the MACHINE-A, operating at a rate of 500 parts per hour.**

In the case of the MACHINE-A in Fig. 5, it can be seen that the trajectories imposed by the cams have almost trapezoidal profiles. This shows up in the accelerations graph, where the peaks at the flexures are marked. This problem is solved with the polynomial profile, which preserves continuity up to the acceleration level with a smoother trajectory. This effect is especially visible in the law of motion of the cylinder.

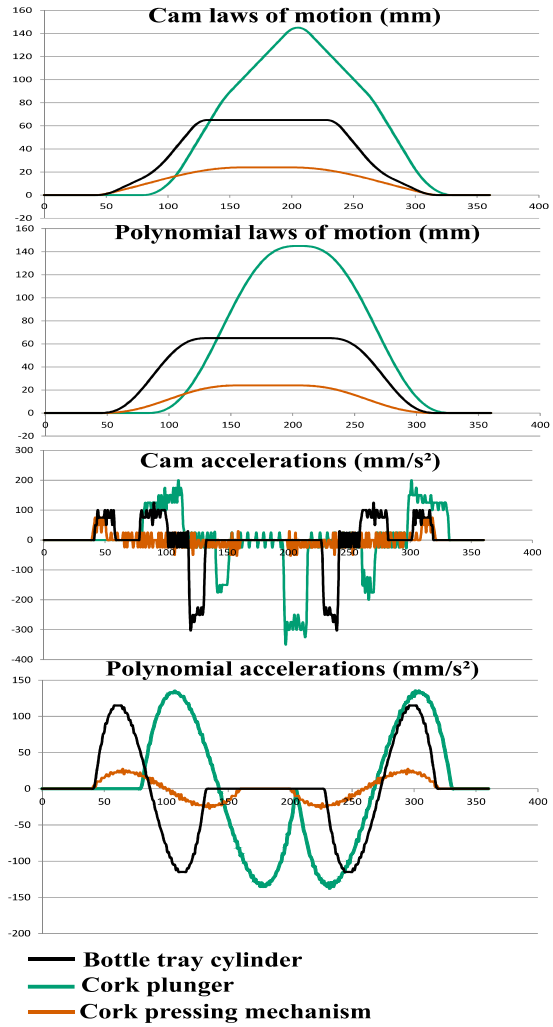


**Fig. 6: Curves of positions and accelerations for the MACHINE B, operating at a rate of 500 parts per hour.**

The MACHINE B in Fig. 6 has the same problems as the MACHINE-A even if in these cases for the cylinder and the plunger, the change of position is carried out using two intermediate speeds, considerably decreasing the peak acceleration values. Also, in this case, the change to the polynomial trajectory reduces the maximum accelerations, although the effect is less noticeable.

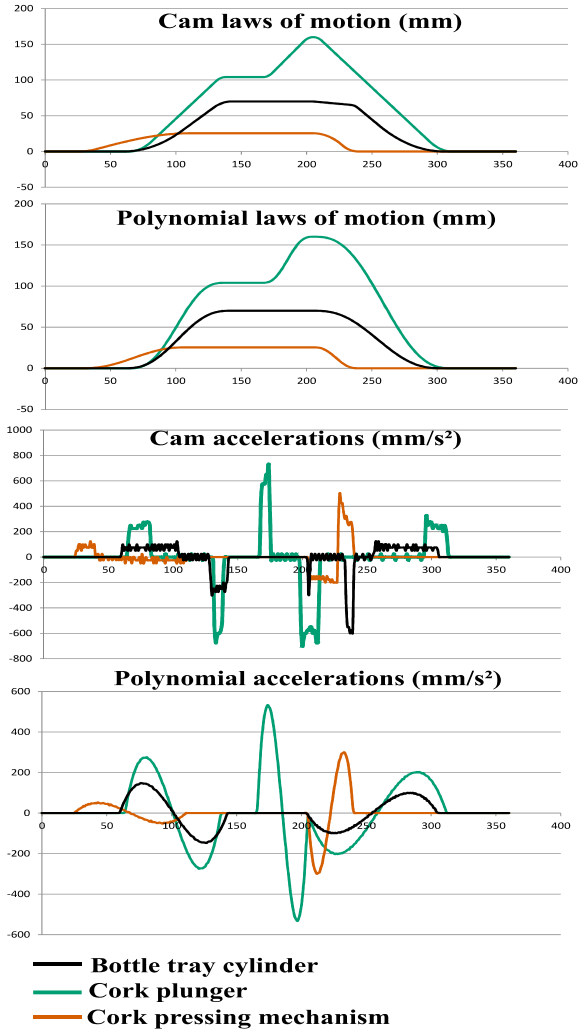


**Fig. 7: Curves of positions and accelerations for the MACHINE C, operating at a rate of 500 parts per hour.**

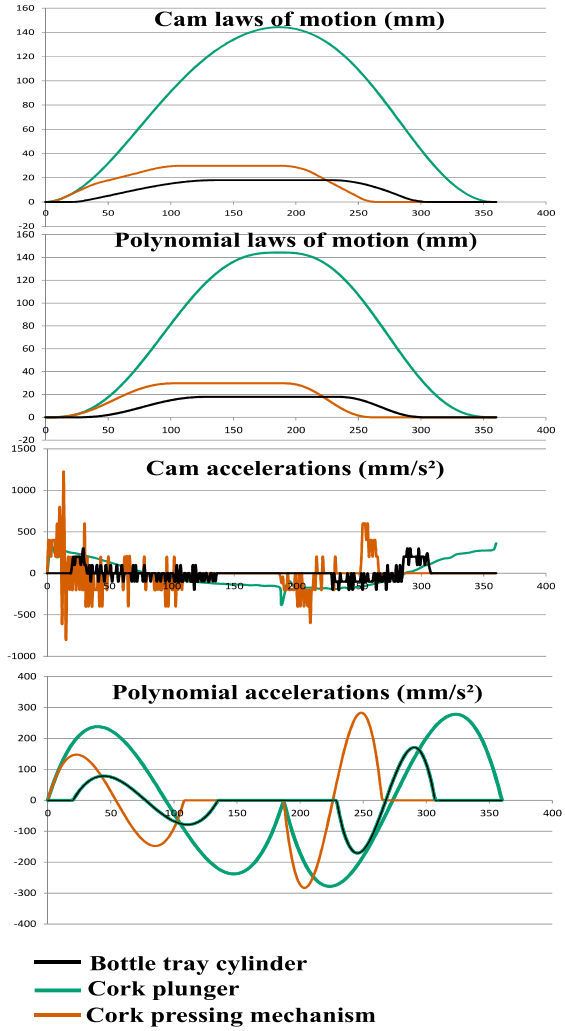


**Fig. 8: Curves of positions and accelerations for the MACHINE D, operating at a rate of 1000 parts per hour.**

The MACHINE C (Fig. 7) has trajectories with more complex shapes, but the position changes always occur with almost trapezoidal profiles, in particular as regards the plunger. This machine, in fact, is equipped with a system of aspiration and addition of inert gas with the aim of improving the preservation characteristics of the bottled product. This, however, requires that, during the capping phase, the cap is kept for a certain time near the mouth of the bottle and then quickly inserted.

In this case, even by using the polynomial trajectory, it is not possible to reduce the peak of acceleration of the plunger because it is necessary to quickly perform two changes of position, and there is not much margin for smoothing.

Unlike previous models, the MACHINE D features only one cam used for the control of the bottle tray cylinder. The plunger mechanism is moved by a rod-crank system, whereas the slide of the compression system is controlled by two levers linked to a splined shaft. Being a single-headed machine, it also has higher operating speeds than the cases seen previously, and this tends to raise the level of the acceleration peaks (Fig. 8).

The greatest criticality, in this case, is due to the slide of the compression system, whose trajectory has an abrupt increase in position at the beginning of the work cycle. As can be seen in the image, this can be definitely mitigated using the polynomial law.

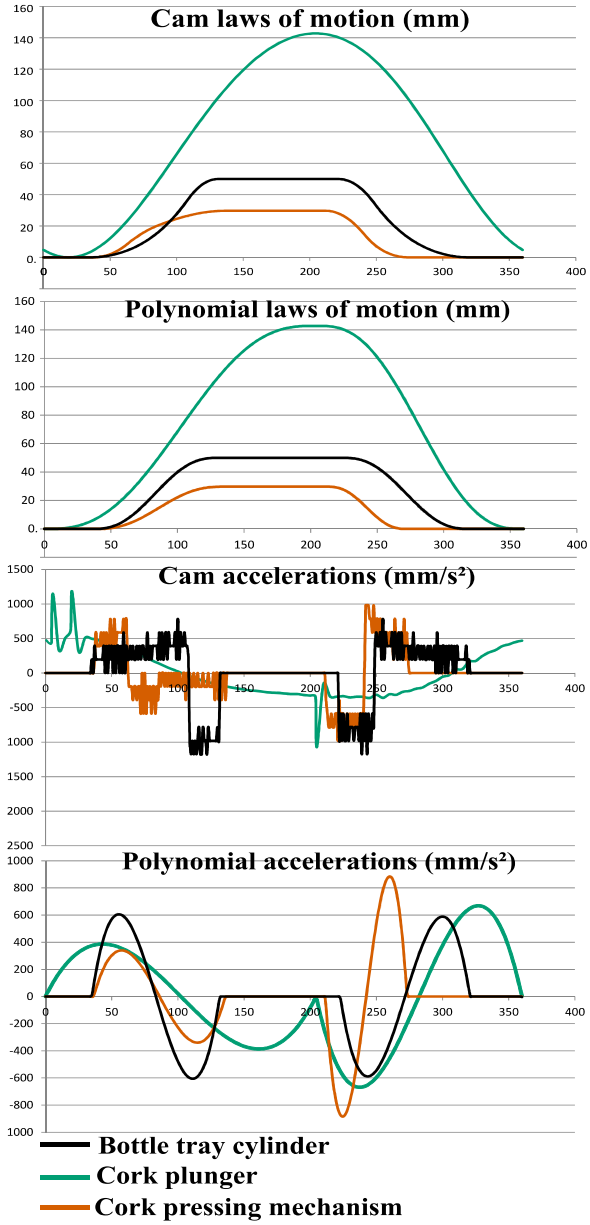


**Fig. 9: Curves of positions and accelerations for the MACHINE E, operating at a rate of 1400 parts per hour.**

The MACHINE E capping machine is a more evolved model than the previous one, the control of the compression system is no longer performed with a splined shaft but has a dedicated cam. The control of the plunger instead is always entrusted to a crank-rod system. Compared to MACHINE D, the thrusts exerted by the cylinder are more problematic, especially at the arrival and departure points from the upper position (Fig. 9). In any case, the new law of motion is effective in attenuating these peaks.

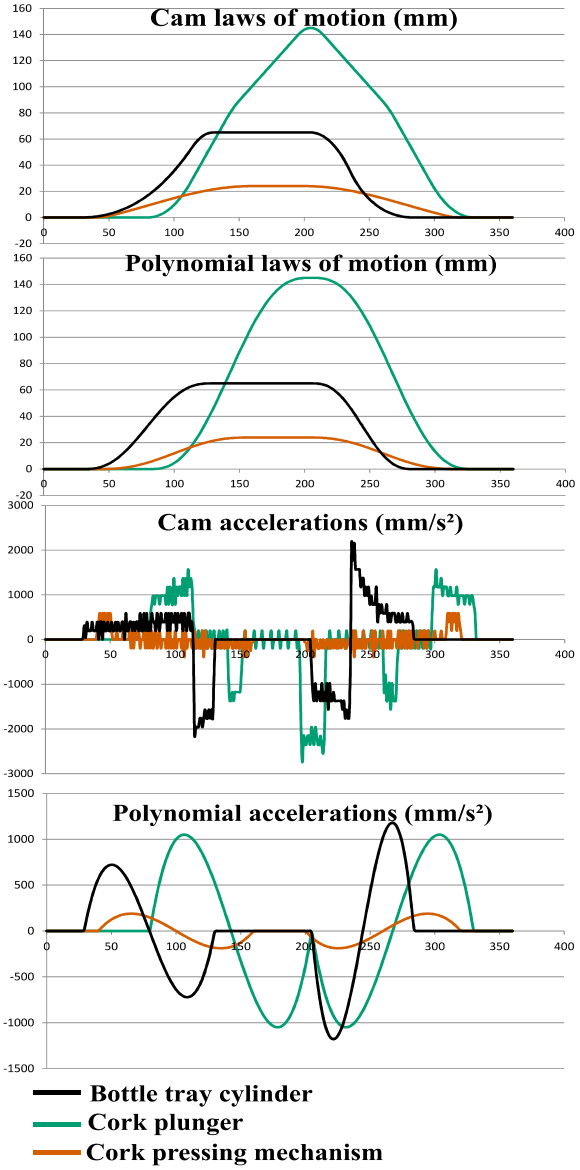


**Fig. 10: Curves of positions and accelerations for the MACHINE F, operating at a rate of 1400 parts per hour.**

The MACHINE E is the only single-head capping machine among those analyzed in which the movements of the parts are all regulated by cams. In this case, the trajectory of the plunger has five sudden changes of speed (Fig. 10) that cause the same situation as seen for MACHINE B. In this case, however, the most critical situation is that of the cylinder. In fact, the cylinder makes two rapid movements in which it reaches a high peak speed and then suddenly slows down. This results in three high peaks in the acceleration graph. The polynomial trajectory brings improvements mainly to the acceleration peaks of the cylinder but has little impact on the other parts.

### *B. Law of motion and load of compression system*

Below are the load and lift diagrams of the compression system at the minimum and maximum speed for each machine[20]. As far as single-head machines are concerned (MACHINE D, MACHINE E, MACHINE F), only one diagram has been shown since the profile of the cam of the slide is identical for each of them. Frequency diagrams on maximum load are also shown, grouped for caps of similar dimensions.

For every cork stopper type, it can be seen that while the cap is kept in compression, the trend of the load exerted is not symmetrical as it should be in an ideal case. In fact, after the first peak, there is a residual force that slowly decreases until the final steep descent (corresponding to the insertion of the cap). This phenomenon is particularly evident for rotary machines operating at low speeds and is due to the spring back of the material after compression. In fact, cork, as well as synthetic materials that imitate its properties, has a time-dependent viscoelastic behavior. Once the cork is compressed, the elastic energy accumulated is slowly released (the process can last hours), and this is a very important factor as it ensures the tightness of the cork stopper once it is bottled [21]. This also explains why this phenomenon is not visible when machines operate at high speed; in fact, in these cases, the elastic return does not have time to manifest itself during the bottling phase, but it is entirely manifested when the cork is already in its seat. The absence of spring back is the reason why there is generally a decrease in the force required for compression as the working speed increases. This effect is especially evident in single-headed machines.

In rotary machines, the small Cork_01 synthetic cork stopper shows moderate spring back at low speed. MACHINE Chas required an increased compression force: the duration of the compression phase is expanded by the presence of the vacuum and inert gas phases, an effect that almost disappears at high speed.

The Cork_02 shows an increase in load in the final compression phase at minimum speed in MACHINE-A and MACHINE B: this is due to the greater resistance that the cap opposes compared to the previous one that is completely coated (Fig. 13). In general, the same phenomena seen in the previous case can be observed.

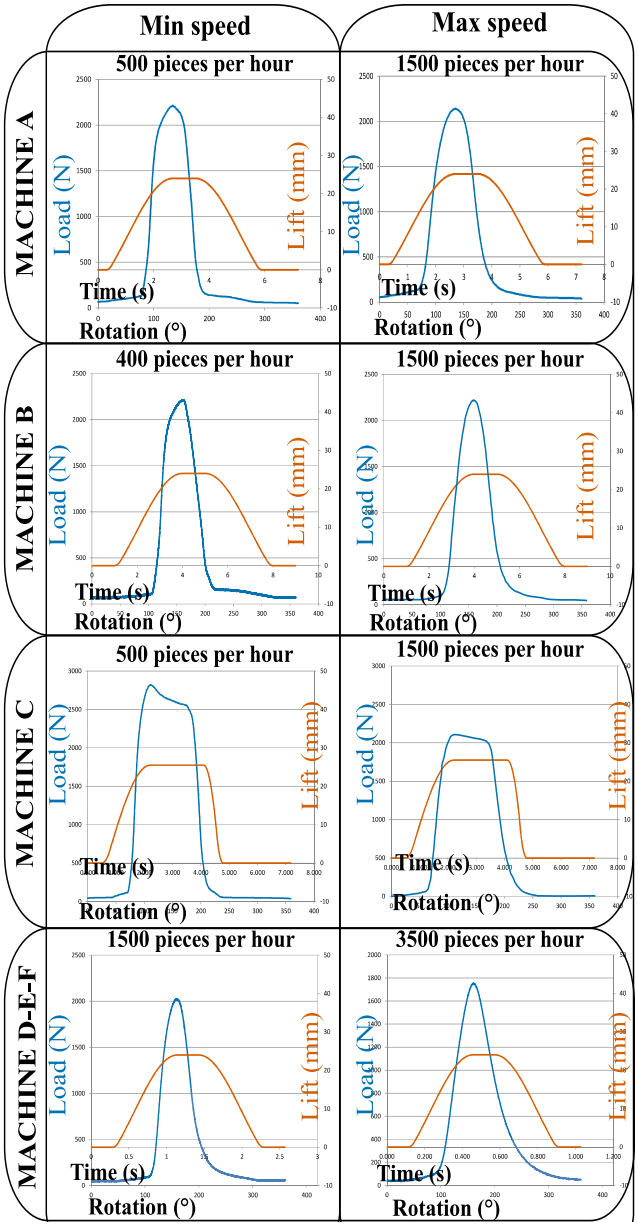


**Fig. 11: Experimental load and lift graphs of the compression slide that moves according to polynomial lawduringCork_01 cap insertion.**

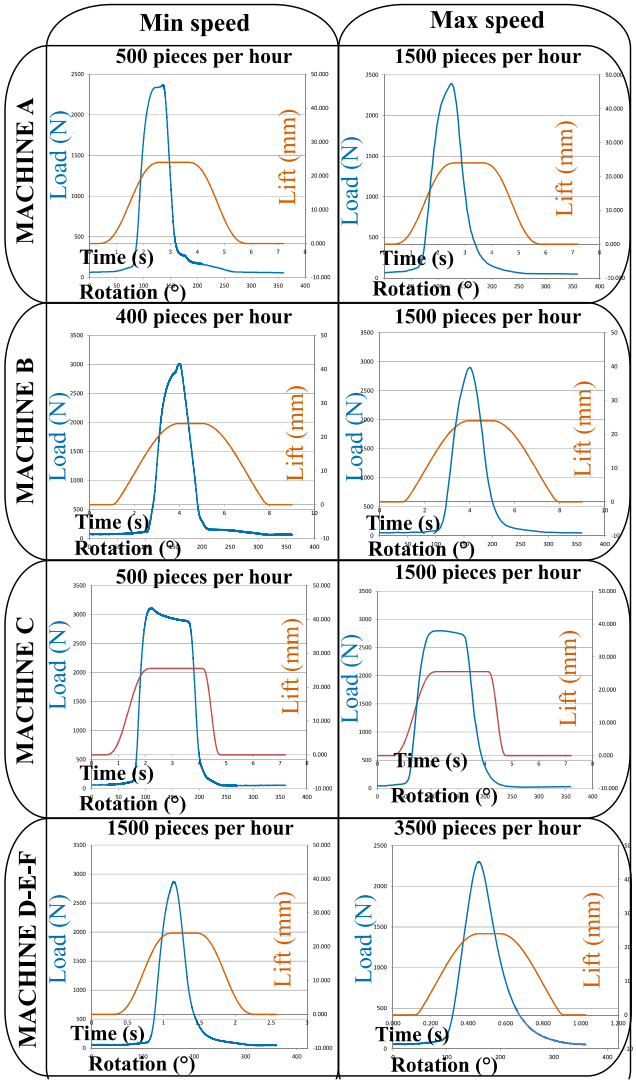


**Fig. 12: Experimental load and lift graphs of the compression slide that moves according to polynomial lawduringCork_02 cap insertion.**

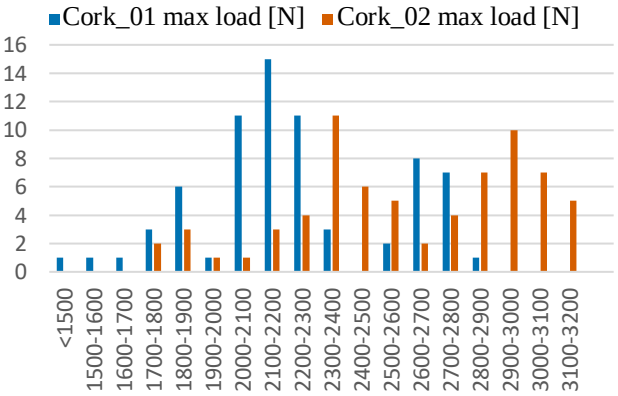


**Fig 13: Frequency graph on maximum load detected during 100 insertions of Cork_01 and 100 insertions of Cork_02**

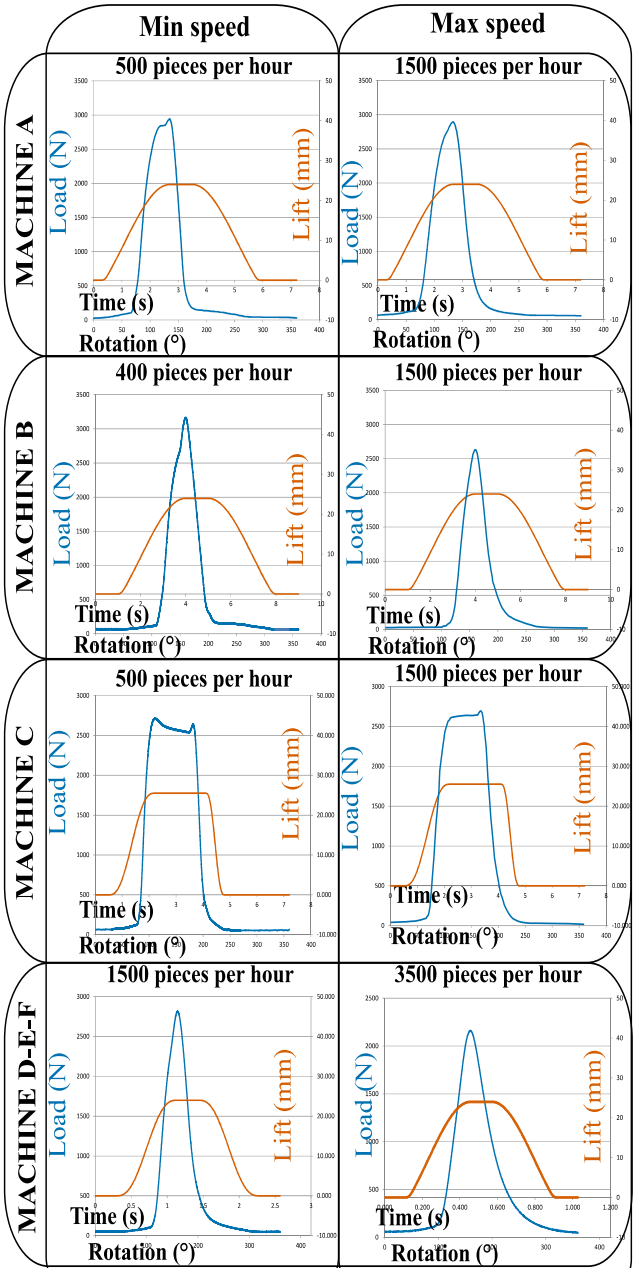


**Fig 14: Experimental load and lift graphs of the compression slide that moves according to polynomial lawduringCork_03 cap insertion.**

In the case shown in Fig. 14, the cap behaves similarly to what was seen in the previous case (Fig. 12) for the same material. One particular aspect is the spike that occurs at the end of the compression phase in MACHINE C. This is believed to be due to a delayed response of the material occurring at high speeds.

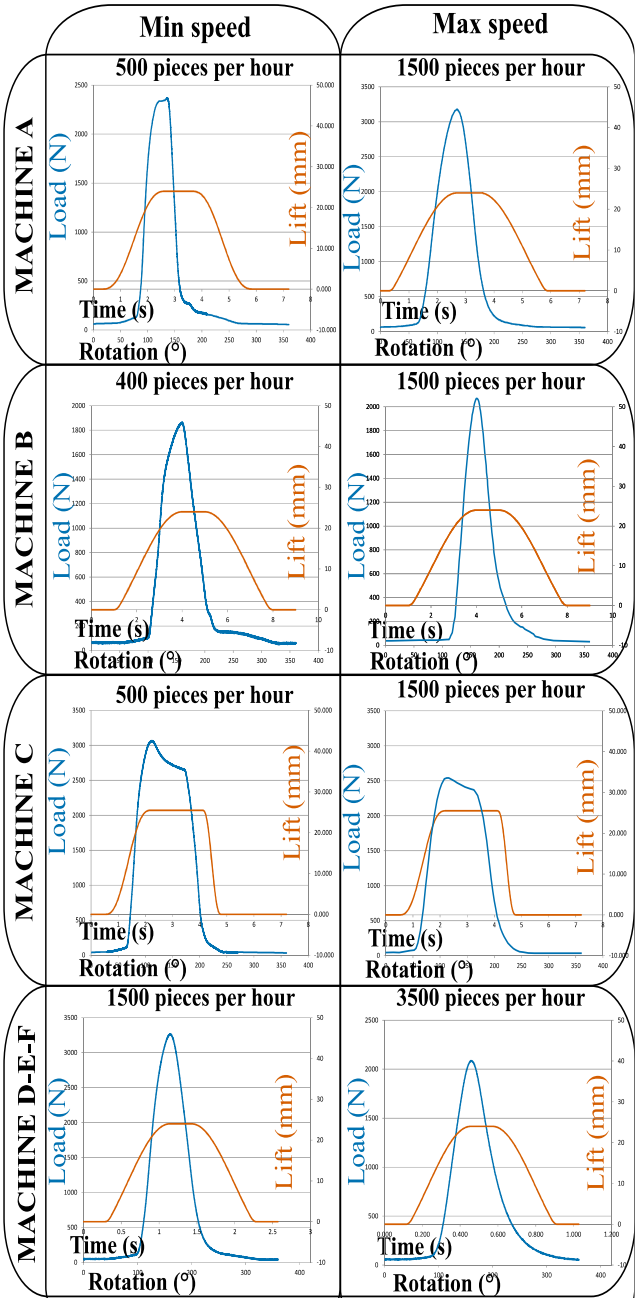


**Fig. 15: Experimental load and lift graphs of the compression slide that moves according to polynomial lawduringCork_04 the cap insertion.**

Natural cork stoppers have a good spring back, which is clearly visible in the graphs. From the tests carried out, it is also the one among the caps with the same size that requires less force for compression (see Fig 17 and table at the end of this paragraph).

In Fig. 16 can be seen that agglomerate stoppers have curves very similar to those of natural cork except for the lesser effect of spring back and the requirement of higher forces (Fig. 17).

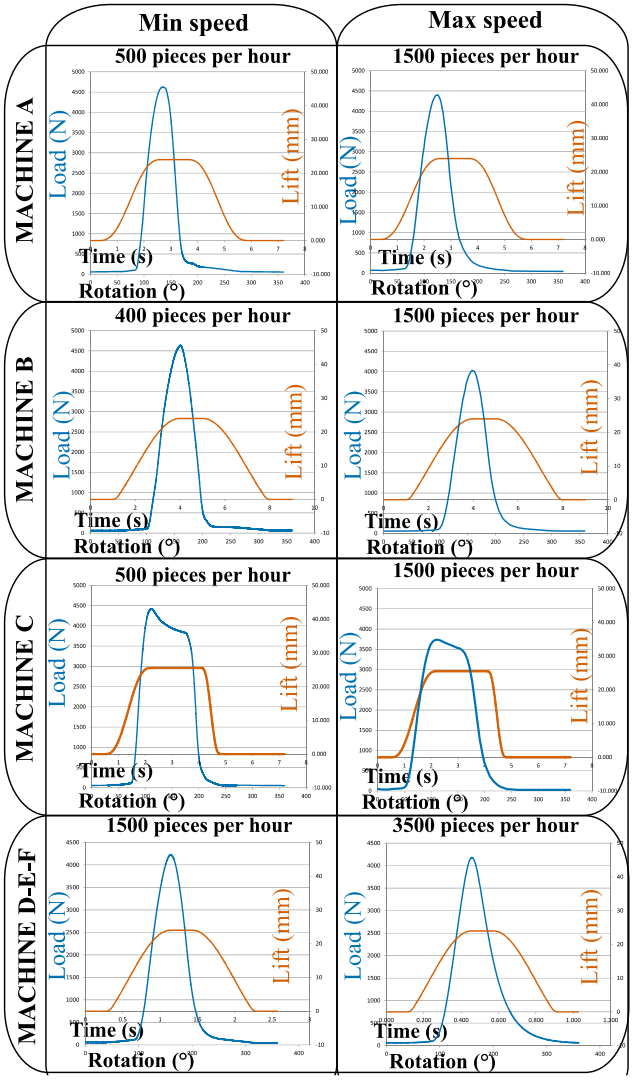


**Fig. 16: Experimental load and lift graphs of the compression slide that moves according to polynomial lawduringCork_05 cap insertion.**

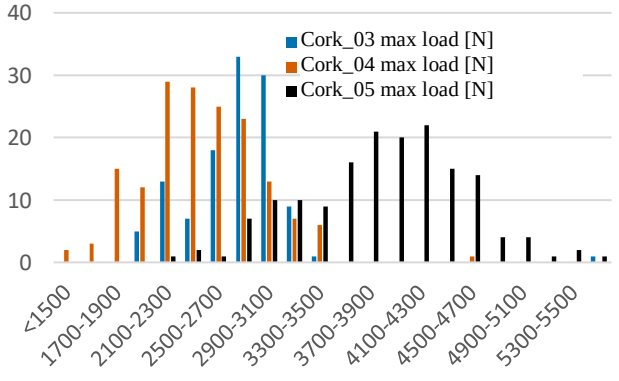


**Fig 17: Frequency graph on maximum load detected during 100 insertions of Cork_03,100 insertions of Cork_04, and 100 insertions of Cork_05**

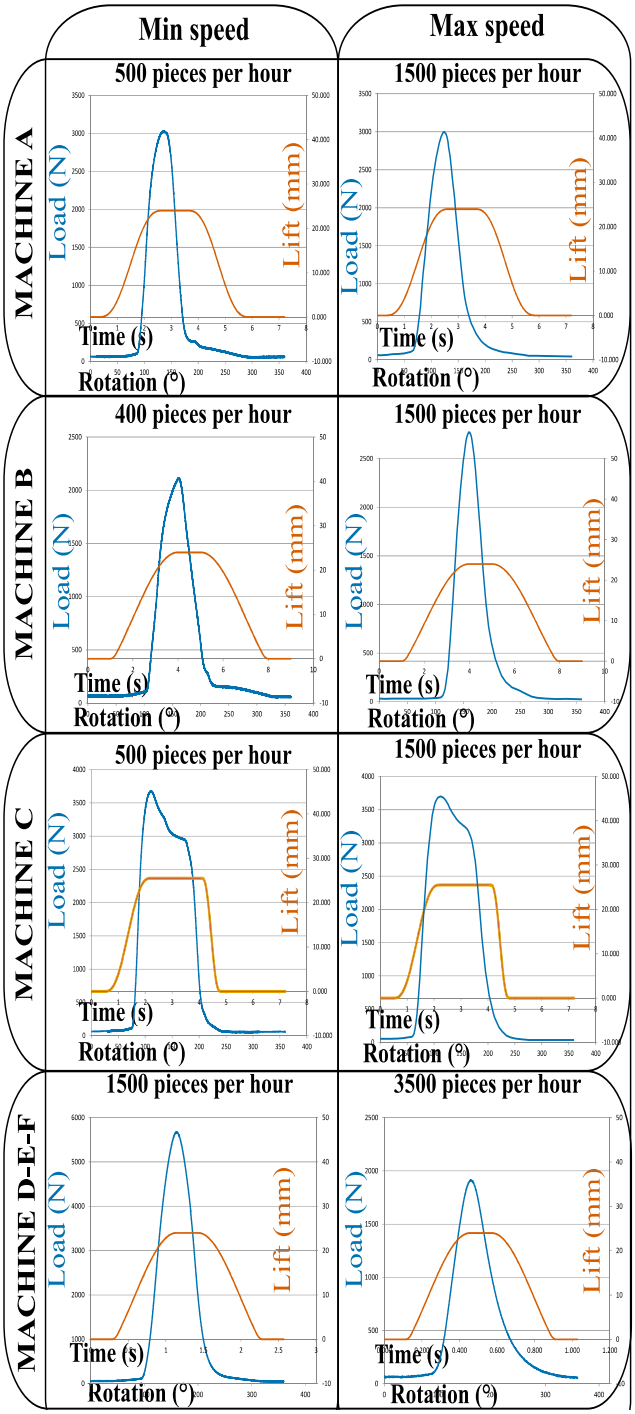


**Fig. 18: Experimental load and lift graphs of the compression slide that moves according to polynomial lawduringCork_06 cap insertion.**

The Cork_06 and Cork_07 large natural cork stoppers have curves (Fig. 18, Fig. 19) that are greatly influenced by the spring-back of the cork, an effect that is enhanced by the diameter and length. The forces required, on average, are lower than those seen for agglomerate corks of lower dimensions.

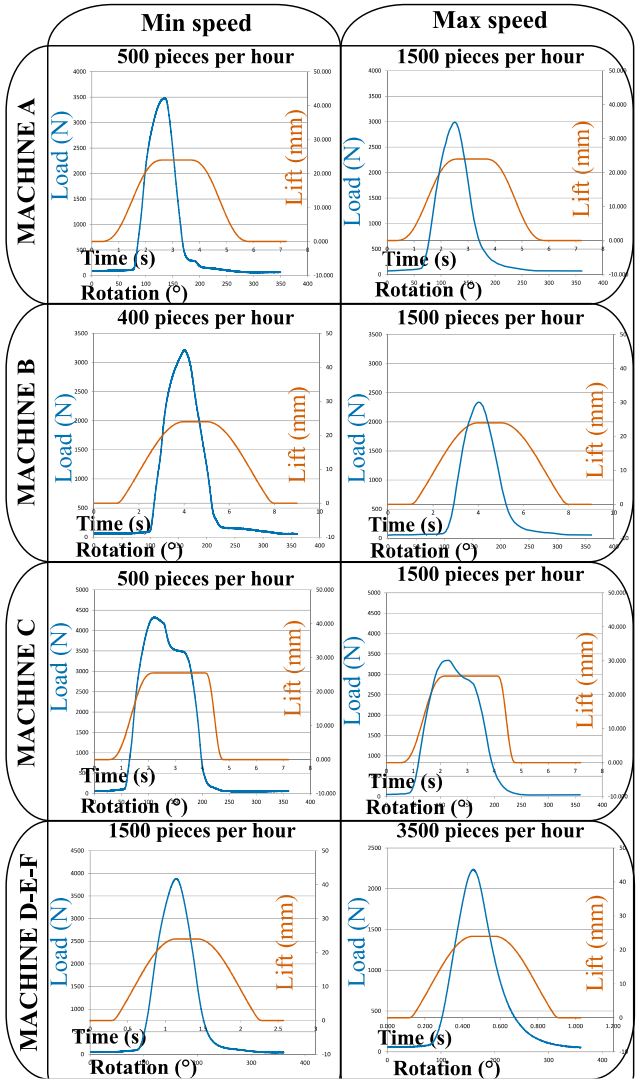


**Fig. 19: Experimental load and lift graphs of the compression slide that moves according to polynomial lawduringCork_07 cap insertion.**

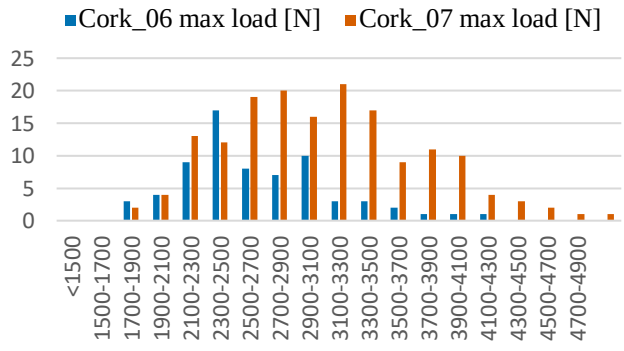


**Fig20: Frequency graph on maximum load detected during 100 insertions of Cork_06 and 100 insertions of Cork_07**

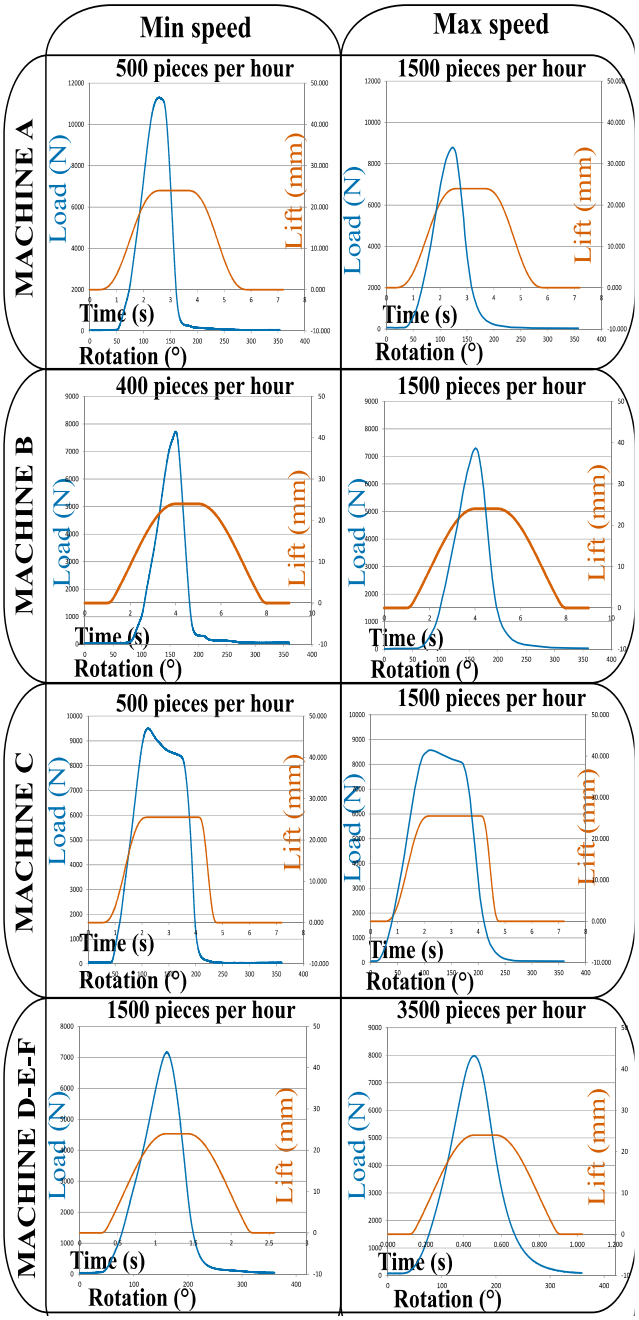


**Fig. 21: Experimental load and lift graphs of the compression slide that moves according to polynomial lawduringCork_08 cap insertion.**

Regarding Cork_08 and Cork_09 caps, it can be observed (Fig. 21, Fig. 22) that the required loads are very similar, although more than doubled compared to what was seen previously. Also, in these cases, it is possible to notice, in general, a decrease in the maximum loads when the machine operates at high speeds.

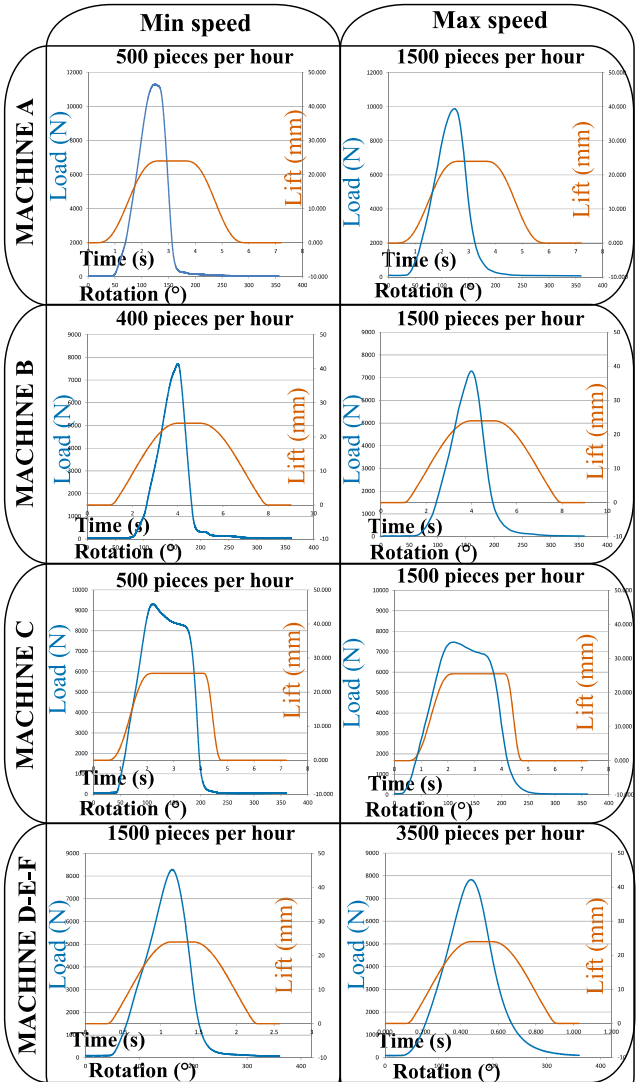


**Fig. 22: Experimental load and lift graphs of the compression slide that moves according to polynomial lawduringCork_09 the cap insertion.**

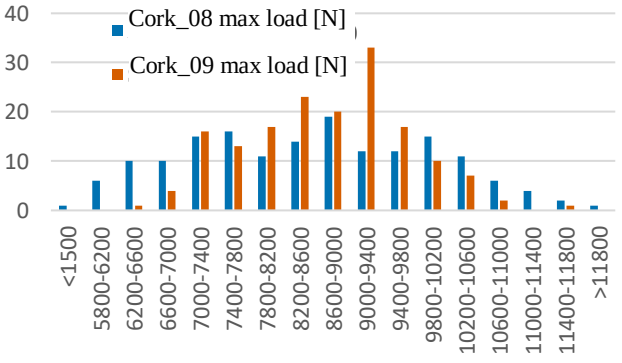


**Fig 23: Frequency graph on maximum load detected during 100 insertions ofCork_08 and 100 insertions of Cork_09**

## IV. CONCLUSIONS

Starting from the study of existing cams used on different capping machine models, it was possible to carry out a kinematic study of acceleration-related stresses. From the experimental results, it is possible to note the improvement in dynamic performance, especially in machines equipped with the simplest cams or those with splined shafts. In these cases, trajectories are definitely smoother, with peaks of lesser amplitude but longer duration. Fair improvements are also obtained on ranges that impose greater compression with more than two levels of lift and intermediate speed variations. On the other hand, the substitution of the law imposed by the connecting rod-crank mechanism with the polynomial one is less effective, as far as the attenuation of acceleration peaks is concerned, since the starting law is already quite smooth [22].

The defined trajectories were then tested using a specially made prototype to verify their effectiveness. These tests also verified the load delivered by the cork compression system for each machine, for various types of cork stoppers, and at different operating speeds. The results showed the correctness of the new polynomial laws and highlighted the effect of the working speed on the duration and intensity of the compression load. In fact, due to the effect of the spring back of the materials used for the caps, in general, there is a request for lower compression forces with increasing speed. The collected data will be useful for the physical realization of the new cams and the dimensioning of the mechanical system.

The next step of this research is to realize the cams with the new profiles and to test them on real machines to verify the performance improvement. Through the use of accelerometers, the trend of vibrations will be measured at various regimes, comparing the new laws of motion with the traditional ones [23] [24]. The dynamic test results also suggest the idea of implementing a speed-dependent law of motion that can take advantage of spring back reduction at high speeds. This modification requires a change in the machine control strategy from a traditional rigid kinematic system to a flexible, controlled kinematic system [25][26] equipped with sensors [27]. Certainly, this transition comes at a cost, but it can serve as a stimulus for the digital transition of the plant in an Industry 4.0 perspective [28][29].

## REFERENCES


[1] F.Y. Chen, A survey of the state of the art of cam system dynamics, Mech. Mach. Theory, 12 (1977) 201–224.

[2] A.M. Shinde, G.J. Tate, R.R. Shinde, S.P. Kadam, P.M. Patil, Design & Manufacturing of Cork Fitting Machine, Irjet., 3 (2016) 2766–2770.

[3] L. Piergiovanni, S. Limbo, Food packaging : materiali, tecnologie e qualità degli alimenti, (2010) 562.

[4] Z. Tang, Y. Li, Y. Zhou, H. Zhang, Inertial vibration characteristics of track chassis caused by the reciprocating motion of crank slider, Shock Vib., 2019 (2019).

[5] S. Bako, T. Usman, I. Bori, A. Nasir, Simulation of a Wet Cylinder Liner, Int. J. Mech. Eng., 6 (2019) 12–17.

[6] R. Garziera, E. Manconi, M. Silvestri, Input laws for dynamic control: Theory, experiments, and robustness, in Proc. 2006 SEM Annu. Conf. Expo. Exp. Appl. Mech., (2006) 1642–1649.

[7] A. Babawuya, I. Bori, M.D. Bako, S.A. Yusuf, A. Jibrin, A.. Elkanah, A. Mohammed, Effects of Generating Plant Noise on Humans and Environment, Int. J. Eng. Trends Technol, 35 (2016) 417–422.

[8] D. Mundo, H.S. Yan, Kinematic optimization of ball-screw transmission mechanisms, Mech. Mach. Theory., 42 (2007) 34–47.

[9] H. Giberti, L. Sbaglia, M. Silvestri, Mechatronic Design for an Extrusion-Based Additive Manufacturing Machine, Mach., 5 (2017) 29.

[10] G. Avventuroso, R. Foresti, M. Silvestri, E.M. Frazzon, Production paradigms for additive manufacturing systems: A simulation-based analysis, in 2017 Int. Conf. Eng. Technol. Innov., IEEE, (2017) 973–981.

[11] G. Avventuroso, M. Silvestri, E.M. Frazzon, Additive Manufacturing Plant for Large Scale Production of Medical Devices: A Simulation Study, IFAC-papers online., 51 (2018) 1442–1447.

[12] C. Wang, X. Wang, B. Zhang, Design of the flying shear servo control system, Proc. - 2017 Chinese Autom. Congr. CAC 2017. 2017-January, (2017) 1659–1664.

[13] S.A. Berestova, N.E. Misyura, E.A. Mityushov, Mechanics of Smooth Coordinated Motion of Multi-Axis Mechatronic Device, Proc. - 2019 Int. Russ. Autom. Conf. RusAutoCon ,. (2019) 1–5.

[14] M.A. Silva, M. Julien, M. Jourdes, P.L. Teissedre, Impact of closures on wine post-bottling development: A review, Eur. Food Res. Technol., 233 (2011) 905–914. https://doi.org/10.1007/S00217-011-1603-9/TABLES/5.

[15] M.A. Fortes, Cork, and Corks, Eur. Rev., 1 (1993) 189–195.

[16] A. Silva, M. Lambri, M.D. De Faveri, Evaluation of the performances of synthetic and cork stoppers up to 24 months post-bottling, Eur. Food Res. Technol, 216 (2003) 529–534.

[17] P. Lopes, C. Saucier, P.-L. Teissedre, Y. Glories, Oxygen transmission through different closures into wine bottles, Pract. Winer. Vineyard.,(2015) 38–42.

[18] H. Venkatesh, K. Annamalai, S. Thiyagarajan, Development of Servo Controlled Automation For Tmc (Tandem Master Cylinder) Performance Test Rig, Int. J. Mech. Eng., 8 (2021) 41–46.

[19] A. Mahmoud M, S. M-Emad S, S. A.B, Vehicle Active Suspension System performance using Different Control Strategies, Int. J. Eng. Trends Technol., 30 (2015) 106–114.

[20] M. Silvestri, M. Confalonieri, A. Ferrario, Piezoelectric actuators for micro-positioning stages in automated machines: experimental characterization of open-loop implementations, FME Trans., 45 (2017) 331–338.

[21] M. Sánchez-González, D. Pérez-Terrazas, Assessing the percentage of cork that a stopper should have from a mechanical perspective, Food Packag. Shelf Life. 18 (2018) 212–220.

[22] D. Groza, C. Antonya, Dynamically Spring Balanced Slider-Crank Mechanism for Reciprocating Machines, Int. J. Mech. Eng., 2 (2015) 22–26.

[23] J.D. Smith, Vibration measurement and analysis, (2013).

[24] P. H. Jain, S. P. Bhosle, A Review on Vibration Signal Analysis Techniques Used for Detection of Rolling Element Bearing Defects, Int. J. Mech. Eng., 8 (2021) 14–29.

[25] H. Giberti, A. Pagani, Flexibility oriented design of a horizontal wrapping machine, Mech. Sci., 6 (2015) 109–118.

[26] M. Silvestri, P. Pedrazzoli, C. Boër, D. Rovere, Compensating high precision positioning machine tools by a self-learning capable controller, Proc. 11th Int. Conf. Eur. Soc. Precis. Eng. Nanotechnology, EUSPEN 2011., 2 (2011) 121–124.

[27] M. Silvestri, M. Banfi, A. Bettoni, M. Confalonieri, A. Ferrario, M. Floris, Use of Laser Scanners in Machine Tools to Implement Freeform Parts Machining and Quality Control, Smart Innov. Syst. Technol., 54 (2015) 527–536.

[28] G. Avventuroso, M. Silvestri, P. Pedrazzoli., A Networked Production System to Implement Virtual Enterprise and Product Lifecycle Information Loops, IFAC-papers online., 50 (2017) 7964–7969.

[29] L. Sbaglia, H. Giberti, M. Silvestri, The Cyber-Physical Systems Within the industry 4.0 Framework, in Mech. Mach. Sci., Springer, Cham, (2019) 415–423.